Designing Highly Sensitive Microwave Antenna Sensor with Novel Model for Noninvasive Glucose Measurements

Abhishek Kandwal[1, 3], Louis W. Y. Liu[2], Jingzhen Li[1], Yuhang Liu[1], Huajie Tang[1], Ziheng Ju[1], Tobore Igbe[4], Rohit Jasrotia[3], and Zedong Nie[1, *]

Abstract—The concentration induced permittivity change involves a dispersion which occurs at the resonant frequency and is often not predictable by simulation using the traditional Cole-Cole model. To overcome this problem, a new Lorentz's model is proposed as a substitute for the Cole-Cole model. Under this new model, the glucose concentration is expected to be measured at the contact interface in the form of a resonant frequency shift. With the help of the model, a contact-based meander-line antenna sensor (CMS) is realized with a high sensitivity of $1.3158\,\mathrm{dB/(mmol/L)}$ in terms of $d|S_{11}|/dC$, or of $17 \sim 18\,\mathrm{MHz/(mmol/L)}$ in terms of $d\omega/dC$. The model has been experimentally validated with in-vitro measurements and for proof-of-concept with in-vivo clinical investigations in the microwave frequency. Consistent with the predictions of model, a linear correlation is observed not only between the resonant frequency shift and the glucose concentration, but also between the S-parameters magnitude and glucose concentration.

1. INTRODUCTION

There is no shortage of research devoted to the field of electromagnetic glucose sensors, in part due to their advantages of being low cost, highly sensitive, flexible, and robust which make them highly capable for industrial use. The microwave sensors have been proposed recently for many biomedical applications including detection at molecular level and for noninvasive glucose measurements in aqueous-glucose solutions and directly over human body [1–11]. In [1, 3, 10], the scattering parameter measurement method was used to conduct glucose sensing on deionized aqueous-glucose solutions and on human subjects with the help of surface plasmonic sensor, split ring resonator, and planar microstrip patch antenna. In [4], a dual band microwave frequency sensor was proposed to test the permittivity variation of different liquid samples including glucose.

The original idea of electromagnetic glucose sensing was based on an assumption that a change of glucose concentration will definitely lead to an observable change in the permittivity. Unfortunately, the reality is not as simple as such. The actual change as a result of a glucose concentration change is often too small to be measurable [26]. Fortunately, several investigations have unanimously revealed that a glucose concentration can manifest as a shift in resonant frequency when sensors were put in direct contact with biomolecules [12–16]. As will be discussed in the sections which follow, the key lies on the effect of dispersion under a surface plasma wave, which is particularly strong when the frequency approaches a resonant frequency [12–16].

Due to the lack of an appropriate model for the permittivity, attempts to verify the measured results by simulation are mostly unsuccessful. Without a proper permittivity model, most of the investigations are limited to in-vitro measurements involving a human blood serum or a glucose-water solution. Very

[1] Shenzhen Institute of Advanced Technology, Chinese Academy of Sciences, Shenzhen 518055, China. [2] Vietnamese German University, Vietnam. [3] School of Physics and Materials Science, Shoolini University, Solan, H.P., India. [4] Center for Diabetes Technology, University of Virginia, VA, USA.

few RF microwave sensors have been successfully used in real-time in-vivo tests over a human body. In [11], for example, a radio frequency patch biosensor was proposed to monitor glucose in aqueous glucose solutions. The experiments provided a sensitivity of 1–2 MHz per mg/dL, but no in-vivo tests were performed. In [12], the authors have provided improved versions of the RF based glucose sensors that provided sensitivity and reusability. Although the tests performed used human serum samples, no direct on-body measurements were done. Another study [13] proposed a coplanar-waveguide and resonant type sensor at the microwave frequencies for the application in biomedical engineering. The sensor in [13] was mainly used to measure solutions with different glucose concentrations. The setup method used was a transmission (S_{21}) measurement method. In [14], the authors proposed a microwave cavity sensor for noninvasive and in-vitro measurements of pig-blood d-glucose. This approach was unique but was not able to achieve a sensitivity comparable to those of other counterparts. There have been some sensors proposed such as epsilon negative resonator or a split-ring resonator for measuring aqueous-glucose solutions. These have not been performed in-vivo tests for proof-of-concept.

In [17, 18], the authors proposed a split ring sensor resonator and a new metamaterial sensor resonator so as to perform aqueous glucose measurements. However, it has been observed that the achieved sensitivities in [17, 18] were not high for in-vivo. In addition, the above-mentioned studies have entirely focused on in-vitro glucose experiments, and no direct on-body testing has been performed. The reason may be simply attributed to the lack of a model that expresses the sensitivity as a function of the glucose concentration.

Recently in [19], a real-time label-free microwave analyzer for the quantitative analysis of glucose concentration was proposed. Using water-glucose solutions, the authors of [19] have achieved a sensitivity of 15.30 dB/g/mL in terms of magnitude change of S_{21} per unit concentration of glucose and 235.32 MHz/g/mL in terms of the resonant frequency shift per unit concentration of glucose. However, the analysis was quantitatively presented with not much theoretical explanation, and no direct in-vivo tests were performed. Some glucose sensing works have been done by other research groups, in which successful in-vitro and in-vivo tests were performed [1, 5, 20–24]. New sensors and multimodal models have been proposed along with in-vivo tests over humans. In addition, works in [29–34] addressed the advances in the use of resonant RF and THz structures for practical biosensing applications, such as proteins, biomolecules, and enzymes.

In this work, a new prediction technique based on a Lorentz's model was developed, and, with the help of this model, a highly sensitive microwave antenna sensor has been photo-lithographically realized and successfully used in an in-vivo experiment. This new glucose sensor adopts the principle of dispersion at interface to increase the sensitivity of the sensing region. The meander shaped design coupled with another structure enhances the sensitivity by confining the fields along the interface between the sensing region and the glucose solution, thereby reducing the leaky losses. The sensor has also exhibited a low detection limit and a linear correlation between scattering parameter measurements and various glucose concentrations.

2. PRINCIPLE, MODEL AND METHOD

2.1. Concept of the Glucose Sensor

Meander line structures have been proven to be able to generate a negative permittivity during a resonance at relatively low frequencies [27]. When a meander line structure is in direct contact with a glucose-loaded sample, which is either a glucose water solution or a solid skin tissue, a surface plasma wave is formed along the interface between the glucose-loaded sample and the meander line structure. This surface plasma wave is always bound to the interface. Due to the presence of this surface plasma wave, an anomalous dispersion occurs at frequencies very close to a resonant frequency. According to [25], the relative permittivity of this glucose-load sample under a surface plasma wave can be calculated using Lorentz dispersion model as given in Equation (1):

$$\frac{\varepsilon}{\varepsilon_0} = 1 + \omega_p^2 \sum_m \frac{s_m/s_o}{\omega_m^2 - \omega^2 - j\omega\gamma_m} \tag{1}$$

where ω_p is the plasma frequency at which electrons oscillate about their equilibrium positions if left to itself. γ_m is the damping coefficient (or loss factor) at the m-th resonance. ω_m is the surface plasmon

resonant frequency for the m-th harmonic. S_m and S_o are respectively the oscillator strengths at the m-th resonance and at the highest resonance.

In a metamaterial, like what was used in this work, the resonant frequencies ω_m, oscillator strengths S_m, and damping coefficients γ_m must be predicted by further models or found experimentally.

During a resonance, the relative permittivity changes as the frequency changes. This phenomenon is known as dispersion. The permittivity change only takes place if and only if the frequency is very close to a surface plasmon resonant frequency, ω_m. When this happens, we have $\approx \omega_m$, and Equation (1) can be rewritten as:

$$\frac{\varepsilon}{\varepsilon_o} = 1 + j\omega_p^2 \frac{S_m/S_o}{\omega_m \gamma_m} \tag{2}$$

In Equation (2), the real part is 1, whereas the imaginary part is a positive number depending on the nature of the metamaterial. In theory, the oscillator strength for a particular resonance S_m can be arbitrarily increased by stacking or repeating multiple unit cells together [28]. With some algebraic manipulation on Equation (2), $d\omega_m/d\varepsilon$ can be expressed as:

$$\frac{d\omega_m}{d\varepsilon} = j\omega_m^2 \left(\frac{S_o \gamma_m}{S_m(\omega_p)^2} \right) \tag{3}$$

As suggested in Equation (3), a change in the complex permittivity will yield a change in the resonant frequency. On the other hand, the sensing sensitivity for a glucose solution can be defined as the total resonant frequency change per glucose concentration change, i.e., $d\omega_m/dC$, where C is the concentration of the glucose solution. $d\omega_m/dC$ can be written as:

$$\frac{d\omega_m}{dC} = \frac{d\omega_m}{d\varepsilon} \frac{d\varepsilon}{dC} \tag{4}$$

Substituting (3) into (4), the sensitivity can be expressed as:

$$\frac{d\omega_m}{dC} = j\omega_m^2 \left(\frac{S_o \gamma_m}{S_m(\omega_p)^2} \right) \frac{d\varepsilon}{dC} \tag{5}$$

where $d\varepsilon/dC$ can be obtained from the Debye model. Over the clinical diabetic range, the real part ε is roughly constant. $d\varepsilon/dC$ should be an imaginary number. Equation (5) has the following implications:

1) The sensitivity is linearly proportional to the loss factor of the glucose solution, γ_m. The Q-factor is given by $Q = 1/\gamma_m$. Hence, according to Equation (5), if the glucose sensor behaves as a metamaterial with no fundamental resonance, then the sensitivity should be inversely proportional to the Q-factor.

2) The imaginary part of $d\varepsilon/dC$ is negative according to the Debye model. $d\omega_m/dC$ is the sensing sensitivity, which according to the Debye model, is expected to be a positive real quantity.

The change in the resonant frequency, $d\omega_m$, can be readily extracted from the scattering parameters S_{21} or S_{11}. If it is S_{11}, then the sensitivity can be expressed as $d|S_{11}|/dC$, with $d|S_{11}|/dC$ given by:

$$\frac{d|S_{11}|}{dC} = \frac{d|S_{11}|}{d\omega} \frac{d\omega}{dC} = \left(\frac{d|S_{11}|}{d\omega} \right) \left(j\omega_m^2 \left(\frac{S_o \gamma_m}{S_m(\omega_p)^2} \right) \frac{d\varepsilon}{dC} \right) \tag{6}$$

$d|S_{11}|/d\omega$ is positive if the resonance in the S_{11} versus frequency plot is a minimum. Hence, when dealing with the resonance in S_{11}, we look for a minimum.

2.2. Hardware of the Glucose Sensor

The proposed glucose sensor was based on a special modified meander topology and was photo-lithographically defined and metalized by physical vapor deposition over a thin silicon wafer. On the top of the silicon substrate is an ultrathin layer of silicon oxide of 0.1 micron thick. The fabrication process was started with preparation of the silicon substrate followed by coating an adhesion layer above it. Then, a negative photo-resist was spin-coated over the substrate. The photoresist was photo-lithographically patterned and exposed through a photomask to the ultraviolet (UV) light.

The fabrication region that was exposed to the ultraviolet light became insoluble in the photo-resist developer. Due to this insolubility, the unexposed region was removed after developing in a developer. In the final step, a conducting metal layer was deposited by physical vapor deposition (PVD). Using the lift off process to remove the photoresist, the copper sensing region was finally obtained. The final sensor design consists of two different structures, including a meander shape and a modified meander shape design.

The unit cells in the meander structure were placed in close vicinity with each other so to enhance the coupling between two structures. In doing so, the surface plasmonic energy over the sensing region was substantially enhanced.

Figure 1 shows the concept of using glucose sensor and its electric field distribution. One end of the glucose sensor was connected to the input source and the other to a matched load termination. As depicted in Fig. 1(a), when a drop of the deionized water-glucose (i.e., 1 μL in volume) was dipped over the sensing region (i.e., coupling points of meander line and T-shape strips), the resonant frequency noticeably increased together with a magnitude change in S_{11}. This change in the S_{11} parameters is a clear indication that the variation of glucose concentrations has induced a rather obvious change in the scattering parameters. This phenomenon can be further highlighted in terms of high field concentrations as shown in Fig. 1(b). Fig. 1(c) shows the S_{11} graph for bare sensor measurement with the deionized
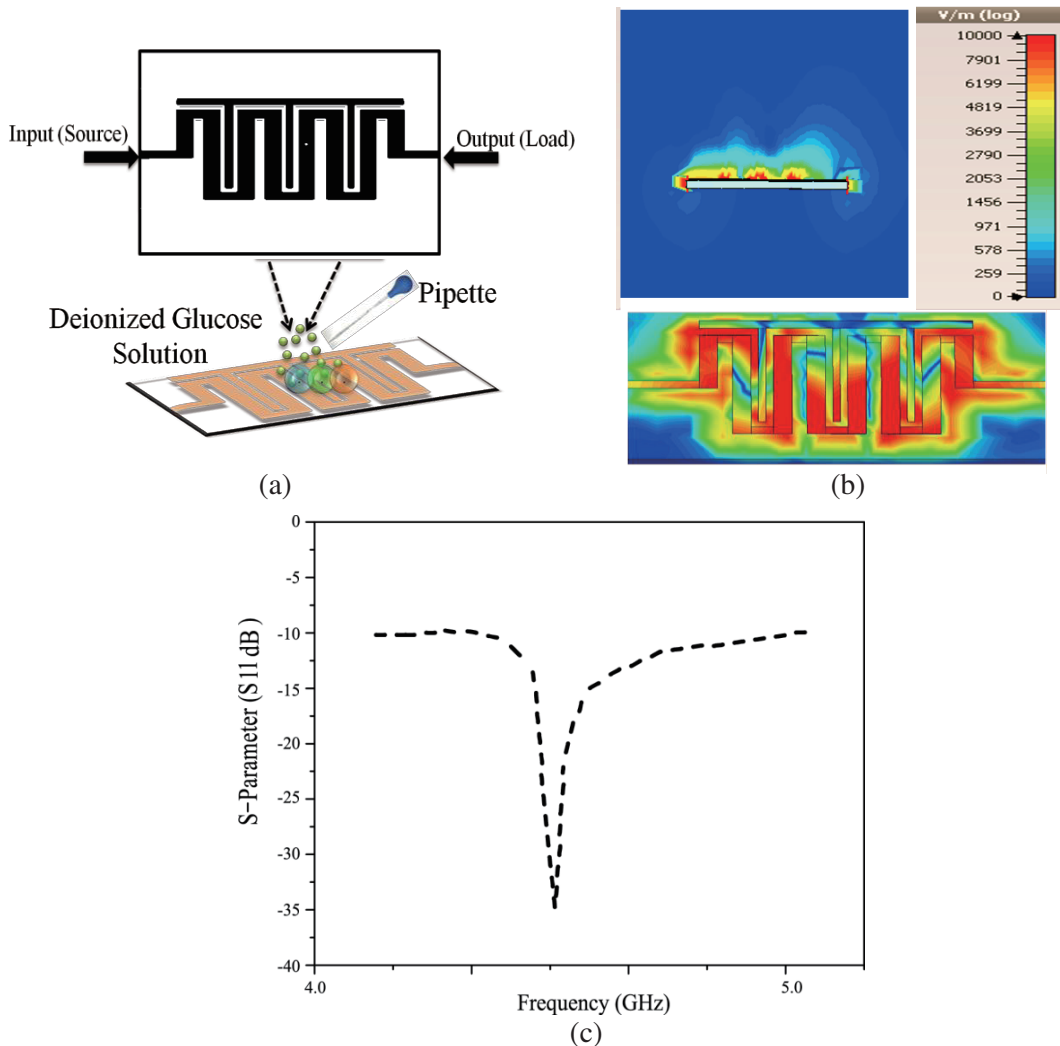
Figure 1. (a) Schematic describing the sensor being tested. (b) Field distribution graph depicting high energy concentration. (c) S_{11} graph for sensor measurement with aqueous-water solution.

aqueous solution with a resonance at 4.5 GHz (in the air without solution is around 7 GHz). The resonance frequency shifts to the left, i.e., from higher frequency to lower one because the medium of contact is changed, i.e., the dielectric constant changes.

The graph in Fig. 1(b), i.e., field distribution graph, has been obtained using a 3D EM simulation software CST Studio Suite. The E-field plot is simulated at 4.5 GHz. The fields are highly confined around the sensing region, which is an indication of maximized surface plasma waves, or equivalently minimized radiation losses. On the other hand, the field coupling means that the energy was stored on the interface between the sensor and the glucose loaded liquid. This stored energy as a result of coupling in the structure has generated a slow wave which yielded a frequency shift in response to a glucose concentration change. The amount of frequency shift depends on the Q-factor as predicted by Equation (5). This fact has been advantageously used to measure and detect the blood glucose levels in in-vitro and in-vivo tests.

2.3. Characterizations: SEM Images, Optical Microscopic Images

Figure 2 depicts the images taken using a scanning electron microscope (SEM). The image displays the thickness of the metal layer that has been deposited during the process of fabrication. A high precision optical microscope was also added to display the top view of the sensing area (see the top of Fig. 2). As can be seen in Fig. 2, the thickness of the substrate material (Si) is 400 microns. A passivation layer of 0.1 microns in thickness. The passivation layer was not clearly visible because its thickness was negligibly thin. A 500 nm thin titanium (Ti) layer was deposited as a seed layer over the substrate and was subsequently thickened by electroplating of copper to a thickness of 2 microns. The overall size of the proposed CMS sensor is 11.4 mm × 6 mm. The dimension of the folded structure was 300 microns by 200 microns, according to the microscopic images. The modified meander line thickness can be seen Fig. 2. The folded meander line is 500 microns thick, and straight meander line is 300 microns thick.
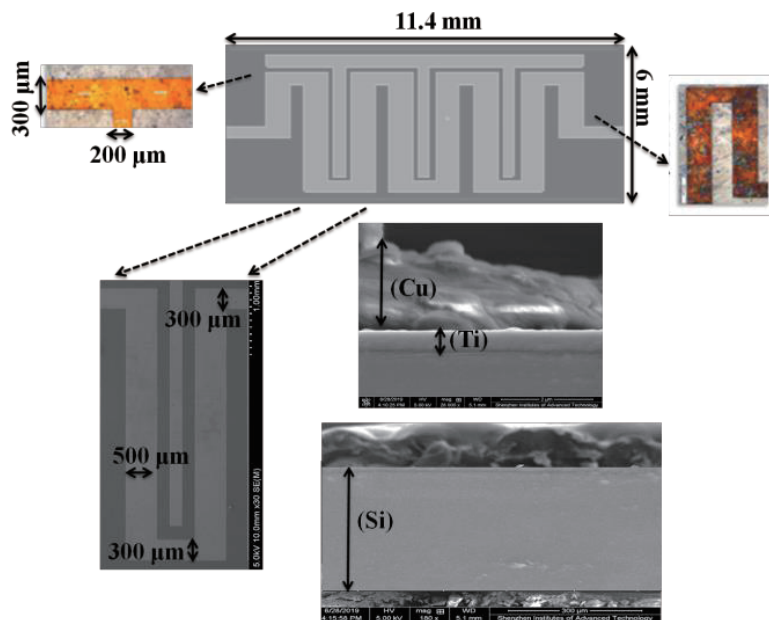
Figure 2. Scanning electron microscope (SEM images) and optical images of the sensor fabricated with dimensions.

3. EXPERIMENTAL RESULTS AND DISCUSSION

This section describes the in-vitro and in-vivo measurements conducted using standard procedures. The proposed CMS sensor was analyzed to estimate the glucose levels in terms of S-parameter measurements

(S_{11} parameter). As will be discussed in the sections which follow, the sensor has exhibited not only an observable magnitude change in the S_{11} parameter but also a clear shift in the resonant frequency for a change in the glucose concentration.

3.1. In-Vitro Measurements

For in-vitro experiments, at first aqueous-glucose solution was prepared by mixing D-glucose powder and deionized-water. By mixing/dissolving glucose powder with a solution of deionized-water, specific glucose concentrations were prepared. The concentration prepared were 2.8 mmol/L, 5.6 mmol/L, 8.3 mmol/L, 11.1 mmol/L, and 16.7 mmol/L that is 0.05, 0.1, 0.15, 0.2, and 0.3 percent by weight, respectively. The proposed range of concentrations from 0.05 to 0.3 percent actually lies within the clinical diabetic range of testing. For a diabetic patient, the range of blood-glucose levels can be anywhere between 0.075 and 0.200 percent, which are respectively equivalent to the 75 mg/dL and 200 mg/dL or 4.3 mmol/L and 11.1 mmol/L, respectively.

In order to analyze the analytical performance of the proposed glucose sensor, the scattering parameters of the sensor in an unloaded condition were first obtained using a vector network analyzer. The frequency range used for testing the bare sensor was from 10 kHz to 10 GHz. During the glucose sensing experiments, the electromagnetic wave from the input port was incident on the prototype under test. Using network analyzer, the S_{11} parameters were measured to determine the levels of reflected and transmitted energy between two ports. Fig. 3(a) depicts the PCB specially fabricated for in-vitro measurements using the proposed CMS sensor with sensing region being in middle. Fig. 3(b) shows how 1 µL (solution drop volume) of sample was dipped using a micropipette onto the sensing area in an experimental setup for these in-vitro tests. The electric field is highly concentrated along the sensor coupling points, so the sensing region can be chosen at the center. The proposed glucose sensor was connected at both ends to the two-port network analyzer and fixed in a stable position with virtually no movement. As opposed to other studies, where a cavity container was needed on the top of the sensing region [11] in a way to fix the volume of the glucose solution, our method was dependent on the contact interface only, and the actual measured results do not vary in terms of S-parameters since we are using very little drop of 1 µL solution which is oozing way.

Figure 4 depicts the results of the in-vitro experiments performed using prepared glucose concentrations. Fig. 4(a) shows the measured scattering parameter (S_{11}) with respect to resonant

(a)

(b)
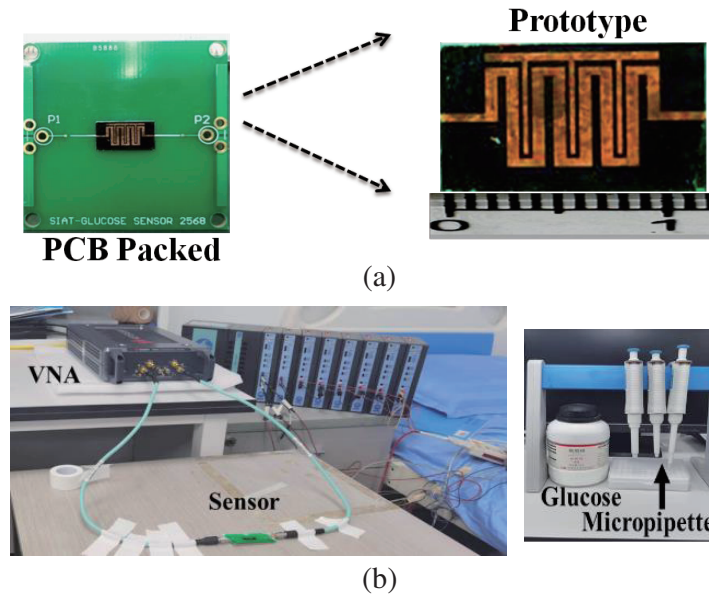
Figure 3. (a) PCB packaging and fabricated prototype of sensor. (b) Setup for In-vitro tests using VNA (left) and Glucose used with micropipettes (right).

frequency (GHz) when the glucose concentration was incremented from $2.8\,\text{mmol/L}$ to $16.7\,\text{mmol/L}$. As the glucose concentration increased, the resonant frequency of the S_{11} dip increased accordingly from $4.7\,\text{GHz}$ to $4.9\,\text{GHz}$. A linear correlation has been observed between the resonant frequency shifts and the prepared glucose concentrations as shown in Fig. 4(b), although the glucose concentration is known to be inversely proportional to the permittivity. Here, the slope represents the sensitivity of the in-vitro measurements, which was 0.0147GHz/mmol/L. Fig. 4(c) shows the S_{11} magnitude graph with increasing glucose concentrations. The measured S_{11} for the glucose concentrations were $-36\,\text{dB}$, $-34\,\text{dB}$, $-32\,\text{dB}$, $-27\,\text{dB}$, and $-24\,\text{dB}$ at different glucose concentrations, respectively. The sensor has achieved a sensitivity of $11\,\text{dB/mmolL}^{-1}$ (in terms of S_{11} magnitude change) and a detection limit below $0.05\,\text{wt.\%}$. Fig. 4(c) also shows the S_{11} result as a function of glucose concentration with error bar for multiple measurements (5-times). This graph clearly shows a highly linear correlation between the magnitude of S_{11} and the resonant frequency, which was exactly what Equation (6) has predicted.
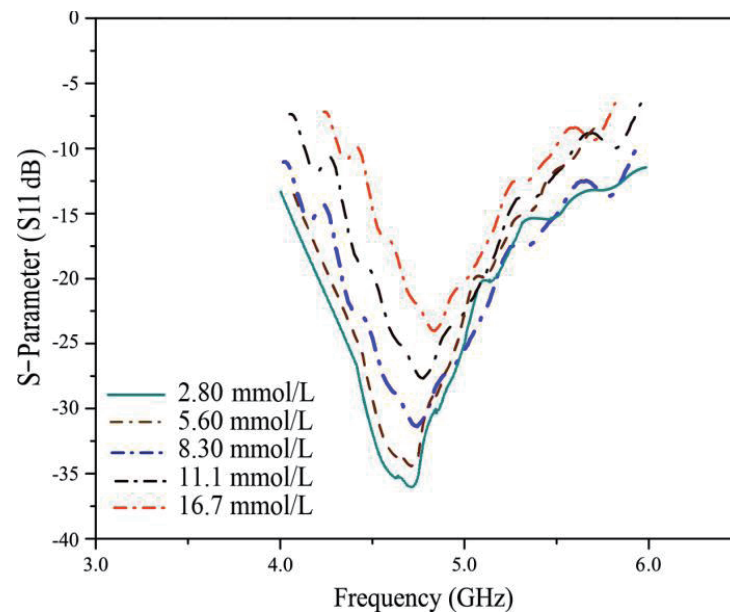
(a)
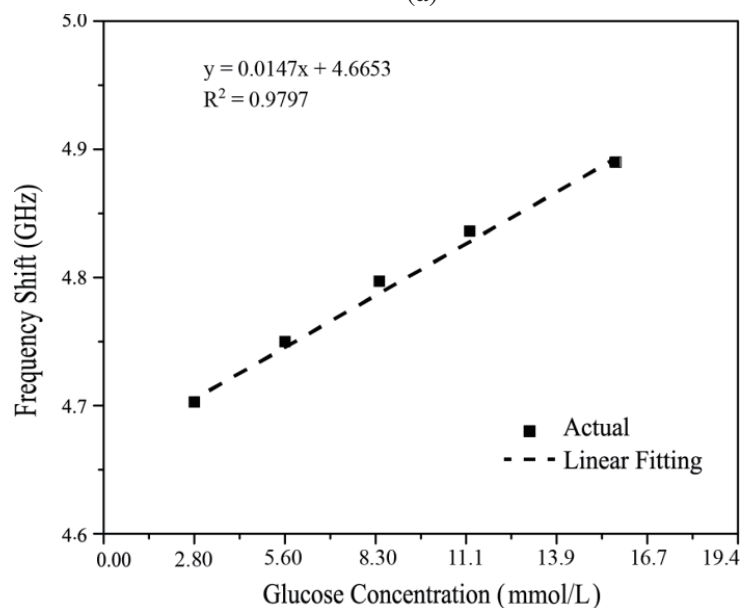
(b)
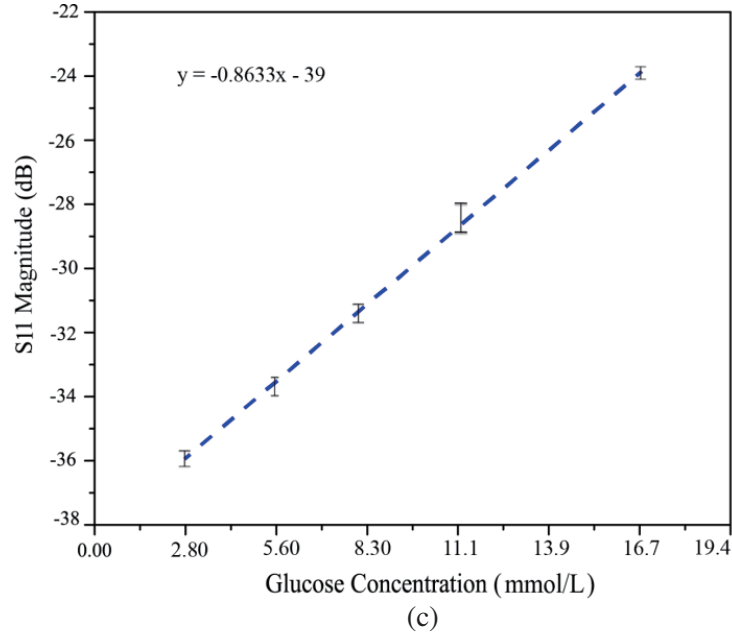
Figure 4. In-vitro tests at different aqueous-glucose concentrations: (a) Variation of S-parameter (S_{11} in dB) with Frequency (GHz). (b) Linear relationship of resonant frequency with glucose concentrations. (c) S_{11} (dB) magnitude variation for glucose concentrations with error bar for multiple measurements.

The change in glucose concentration results in a change of the effective permittivity, which in turn leads to a linear change in the magnitude of S_{11} parameter.

3.2. In-Vivo Measurements over the Human Subjects

In order to further validate the model and in-vitro measurements and observe the effect of sensor over the human body, in-vivo tests have been performed at the Shenzhen Institutes of Advanced Technology (SIAT), Chinese Academy of Sciences (CAS). Five volunteers of different age groups have taken part in the investigations (five healthy male and female volunteers). All the subjects have given their consent in order to perform the experiments over them. These experiments were approved by SIAT CAS ethics committee and were done in accordance with the set relevant regulations and guidelines. The measurements have been carefully conducted.

Figure 5 shows the experimental setup for in-vivo tests over the human subjects. The proposed CMS glucose sensor was tightly fastened over the right arm/forearm of each human subject, and the arm was fixed at one point. The sensor was connected on another end using two port connectors to the
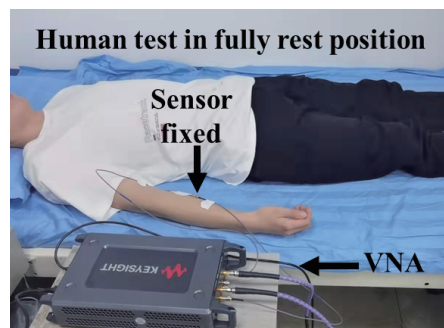
Figure 5. Experimental setup for in-vivo tests: Sensor attached to right arm.

vector network analyzer. The connections were tightened to eliminate unwanted errors or fluctuations during the measurements. In every in-vivo measurement, the sensor was first calibrated to the starting point. Each human subject was put in a steady state condition in a clean room in order to avoid any error due to movements or external interferences.

To start the experiment and observe the effect of varying glucose levels on the scattering parameter (S_{11}), an oral glucose tolerance test (OGTT) was performed. The experiment started at 8:00 AM each day, and during the whole duration of measurement, the subject was being rested in a stable position without any physical movement. The subject was asked to drink a 75 gm of anhydrous glucose-solution before the actual OGTT test. A blood strip device, i.e., ACCU-CHEK meter, was used to take out a little blood drop from the left hand index finger of the subject at regular intervals to check the glucose levels and for validation checks. Along with this, the transmission S_{11} parameters were measured continuously, and readings were regularly noted at an interval of 25 minutes by connecting the proposed CMS sensor to the VNA instrument.

Figure 6 depicts the results of multiple in-vivo measurements done at the glucose concentrations carefully chosen to match with the conditions of the in-vitro tests. Fig. 6(a) shows the variation of S_{11} parameters with frequency at different glucose concentrations. As plotted in Fig. 6(b), resonant frequency shifts achieved have been observed and recorded within the clinical diabetic range. The resonant frequencies obtained are respectively 4.74, 4.765, 4.79, and 4.85 GHz for glucose levels of 5.1 mmol/L, 6.2 mmol/L, 7.3 mmol/L, 8.7 mmol/L, and 9.1 mmol/L. Fig. 6(b) also depicts the positive and linear correlation between the frequency shifts and the glucose concentration. According to the slope of the line in Fig. 6(b), the sensitivity of the in-vitro measurements was 0.0268 GHz/mmol/L. Fig. 6(c) shows the magnitudes of the measured S_{11} at resonances of Fig. 6(a) versus glucose concentrations, together with error bars calculated from multiple measurements performed over five subjects. Similar to Fig. 4(c), Fig. 6(c) also exhibits a highly linear correlation between the magnitude of S_{11} and the glucose concentration. This result validates the reproducibility with high precision and accuracy.

Consistent with the prediction of Equation (6), the transmission measurements have displayed a highly linear change in S_{11} parameter, which partially proves the sensitivity of the proposed CMS sensor during in-vitro tests. Within the clinical diabetic range at different glucose levels of 5.1 mmol/L, 6.2 mmol/L, 7.3 mmol/L, 8.7 mmol/L, and 9.1 mmol/L, the change in S_{21} was respectively -29 dB, -28 dB, -27 dB, -25 dB, and -24 dB. These transmission measurements prove the fact that the sensor has achieved a sensitivity of 1.3158 dB/(mmol/L) in terms of $d|S_{11}|/dC$. For each volunteer, we have chosen the forearm area where the fat tissue is known to be less. We have also tightened the fastener attached to the sensor in a way to force the blood to flow to the sensing area of the CMS sensor. This method is similar to the suction method published in [20, 21].

(a)

$$y = 0.0268x + 4.5995$$
$$R^2 = 0.9888$$

(b)

$$y = -1.3158x - 29.25$$

(c)
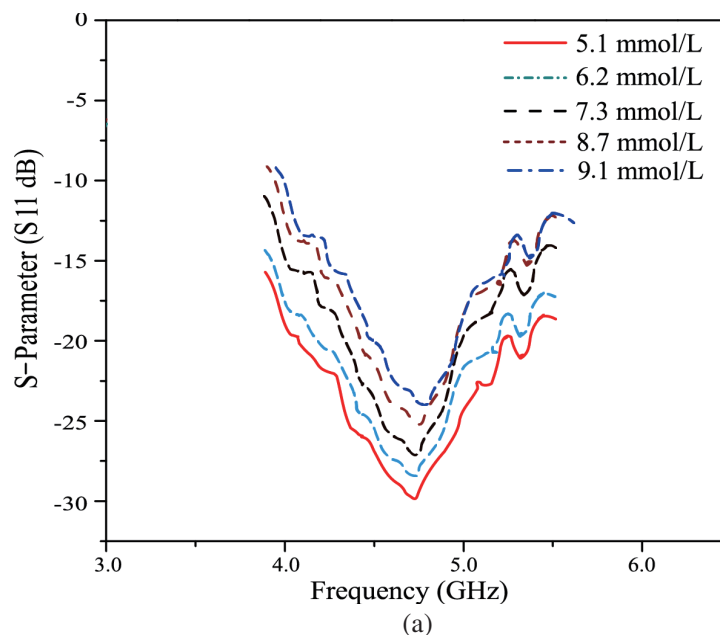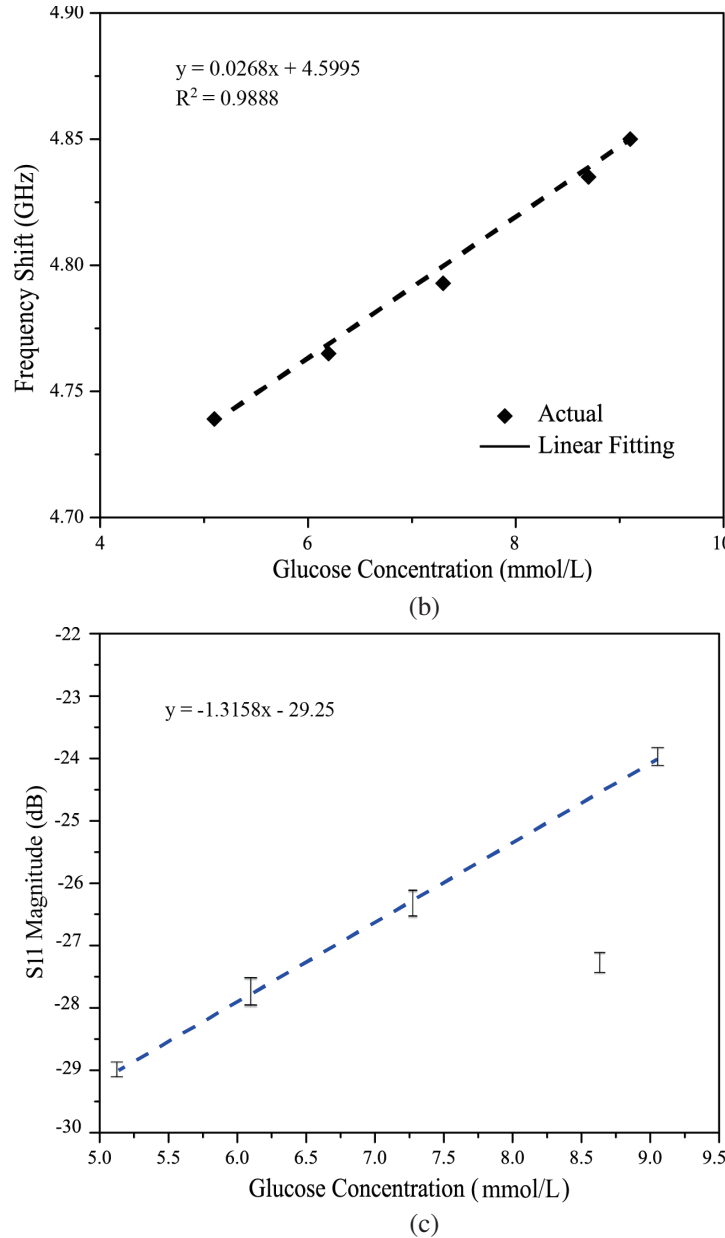
Figure 6. In-vivo tests over human subjects: (a) Variation of Scattering parameter (S_{11} in dB) with frequency (GHz). (b) Linear relationship of frequency with glucose concentrations. (c) S_{11} (dB) magnitude variation for glucose concentrations with error bar for multiple measurements.

Table 1 shows a comparison between other published studies (which have done blood tests or in-vivo tests) and our proposed CMS sensor design. Only a few papers have provided measurements with human blood serum (RML: rectangular meander line sensor), pig blood (MW cavity: microwave cavity sensor) or over human body (square patch sensor). Some of the works, i.e., [1, 23], based on reflection (S_{11}) measurement method using human subjects have also been compared in the table. As can be clearly seen from the table, our proposed CMS sensor has exhibited very good properties for direct in-vivo tests over human body. In this work, an excellent sensitivity has been obtained along with low detection limit. The proposed CMS sensor has not only provided high linear correlation in terms of frequency shift of S_{11} parameter but also shown a high linear correlation in terms of return loss (dB) of reflection coefficient S_{11}.

Table 1. Comparison with counterparts.

Ref.	Sensor	Freq. (GHz)	Sensitivity (Change in S_{21} or S_{11} per unit glucose level)	Lowest Detection Limit	On-body (In-vivo)
[1]	SPP	~ 8	$\Delta = 1.03$ dB/(mmol/L)	$50\,\text{mg/dl}$	Yes (Human body)
[3]	SRR	$\sim 1\text{--}6$	3.45 dB/(mg/ml)	$70\,\text{mg/dl}$	Yes (Blood)
[4]	SRR	$\sim 5\text{--}8$	0.28%	$0.2\,\text{g/ml}$	No (Solutions)
[10]	Square Patch	~ 60	$\Delta = 0.0116$ dB/(mmol/L)	$0.025\,\text{wt.\%}$	Yes (Human body)
[12]	RML	~ 9.2	$\Delta = 0.00113 \sim 0.002$ dB/(mg/dL)	$8.01\,\text{mg/dl}$	No (Human blood Serum)
[14]	MW Cavity	~ 4.75	$\Delta = 0.016$ dB/(mg/dL)	N/A	No (Pig blood)
[23]	SRR	$\sim 2\text{--}3$	$\Delta = 0.734$ dB/(mmol/L)	$0.05\,\text{wt\%}$	Yes (Human body)
Our work	CMS	$\sim 4.5\text{--}5$	$\Delta = 1.3158$ dB/(mmol/L)	$> 0.055\,\text{wt.\%}$	Yes (Human body)

4. CONCLUSION

A new Lorentz's model was proposed as a substitute for the traditional Cole-Cole model with a highly sensitive microwave sensor for glucose sensing to account for the effect of dispersion in the neighborhood of a resonant frequency. Under this new model, the glucose concentration was expected to be measured at the contact interface between the sensing area and the sample and in the form of a resonant frequency shift. The usefulness of the model was demonstrated by realizing a contact-based meander-line sensor with a sensitivity of $1.3158\,\text{dB/(mmol/L)}$ in terms of $d|S_{11}|/dC$, or of $17 \sim 18\,\text{MHz/(mmol/L)}$ in terms of $d\omega/dC$, where C is the concentration of glucose in a solution. The antenna sensor has efficiently detected the glucose concentrations in deionized water-glucose solutions with the lowest detection limit below $0.05\,\text{wt\%}$. The model has been experimentally validated by in-vitro measurements with deionized aqueous-glucose solutions and with in-vivo clinical investigations on 5 human subjects at frequencies between $4.5\,\text{GHz}$ and $5\,\text{GHz}$. The measured results were consistent with the predictions by this model, with a positive and linear correlation noticeably observed between the resonant frequency shift and the glucose concentration, and between $|S_{11}|$ and the glucose concentration. The proposed glucose sensor has achieved, with the help of this model, a sensitivity considerably higher than those of other counterparts. It can be further implemented on system level or extended to an array design with more compact dimensions to perform real time human body non-invasive blood monitoring.

5. CONFLICT OF INTEREST AND ETHICS STATEMENT

Authors declare no conflict of interest. Informed consent has been taken from all the subjects/volunteers for performing experiments in accordance with relevant ethics &guidelines.

ACKNOWLEDGMENT

REFERENCES

1. Kandwal, A., Z. Nie, T. Igbe, J. Li, Y. Liu, L. Liu, and Y. Hao, "Surface plasmonic feature microwave sensor with highly confined fields for aqueous-glucose and blood-glucose measurements," *IEEE Transactions on Instrumentation and Measurement*, Vol. 70, 1–9, 8000309, 2021.

2. Blazquez-Bello, S., Y. Campos-Rocaa, A. Bangertb, and C. Sandhagen, "Impact of substrate and bending angle on the performance of microwave PCB sensors for permittivity measurements," *Measurement*, Vol. 175, 109114, 2021.

3. Omer, A. E., G. Shaker, S. Safavi-Naeini, et al., "Non-invasive real-time monitoring of glucose level using novel microwave biosensor based on triple-pole CSRR," *IEEE Transactions on Biomedical Circuits and Systems*, Vol. 14, No. 6, 1407–1420, 2020.

4. Kiani, S., P. Rezaei, and M. Navaein, "Dual-sensing and dual-frequency microwave SRR sensor for liquid samples permittivity detection," *Measurement*, Vol. 160, 107805, 2020.

5. Li, J., T. Igbe, Y. Liu, Z. Nie, et al., " An approach for noninvasive blood glucose monitoring based on bioimpedance difference considering blood volume pulsation," *IEEE Access*, Vol. 6, 51119–51129, 2018.

6. Ishimaru, A., *Electromagnetic Wave Propagation, Radiation, and Scattering: From Fundamentals to Applications*, John Wiley Sons, 2017.

7. Karacolak, T., E. C. Moreland, and E. Topsakal, "Cole-cole model for glucose dependent dielectric properties of blood plasma for continuous glucose monitoring," *Microw. Opt. Technol. Lett.*, Vol. 55, 2013.

8. Yilmaz, T., R. Foster, and Y. Hao, "Broadband tissue mimicking phantoms and a patch resonator for evaluating noninvasive monitoring of blood glucose levels," *IEEE Transactions on Antennas Propag.*, Vol. 62, 3064–3075, 2014.

9. Yilmaz, T., R. Foster, and Y. Hao, "Towards accurate dielectric property retrieval of biological tissues for blood glucose monitoring," *IEEE Transactions on Microw. Theory Tech.*, Vol. 62, 3193–3204, 2014.

10. Saha, S., H. Cano-Garcia, I. Sotiriou, et al., "A glucose sensing system based on transmission measurements at millimetre waves using microstrip patch antennas," *Sci. Reports*, Vol. 7, 6855, 2017.

11. Qiang, T., C. Wang, and N.-Y. Kim, "Quantitative detection of glucose level based on radiofrequency patch biosensor combined with volume-fixed structures," *Biosensors and Bioelectronics*, Vol. 98, 357–363, 2017.

12. Kim, N. Y., R. Dhakal, K. K. Adhikari, E. S. Kim, and C. Wang, "A reusable robust radio frequency biosensor using microwave resonator by integrated passive device technology for quantitative detection of glucose level," *Biosensors and Bioelectronics*, Vol. 67, 687–693, 2015.

13. Maosn, A., A. Shaw, and A. Al-Shamma, "A co-planar sensor for biomedical applications," *Procedia Engineering*, Vol. 47, 438–441, 2012.

14. Kim, S., H. Melikyan, J. Kim, A. Babajanyan, J.-H. Lee, L. Enkhtur, B. Friedman, and K. Lee, "Noninvasive in vitro measurement of pig-blood d-glucose by using a microwave cavity sensor," *Diabetes Research and Clinical Practice*, Vol. 96, No. 3, 379–384, 2012.

15. Kandwal, A., J. Li, T. Igbe, et al., "Young's double slit method-based higher order mode surface plasmon microwave antenna sensor: Modeling, measurements, and application," *IEEE Transactions on Instrumentation and Measurement*, Vol. 71, 1–11, 2022.

16. Choi, H., J. Naylon, S. Luzio, et al., "Design and in vitro interference test of microwave noninvasive blood glucose monitoring sensor," *IEEE Transactions on Microw. Theory Tech.*, Vol. 63, 3016–3025, 2015.

17. Camli, B., E. Kusakci, B. Lafci, et al., "A microwave ring resonator based glucose sensor," *Procedia Eng.*, Vol. 168, 465–468, 2016.

18. Islam, M., A. Hoque, A. Almutairi, and N. Amin, "Left-handed metamaterial-inspired unit cell for S-band glucose sensing application," *Sensors*, Vol. 19, 169, 2019.

19. Abedeen, Z. and P. Agarwal, "Microwave sensing technique based label-free and real-time planar glucose analyzer fabricated on FR4," *Sensors and Actuators A: Physical*, Vol. 279, 132–139, 2018.

20. Liu., L. W. Y., A. Kandwal, Q. Cheng, et al., "Non-invasive blood glucose monitoring using a curved goubau line," *Electronics*, Vol. 8, 662, 2019.

21. Liu., L. W. Y., A. Kandwal, A. Kogut, et al., "In-vivo and ex-vivo measurements of blood glucose using whispering gallery modes," *Sensors*, Vol. 20, 830, 2020.

22. Tobore, I., J. Li, A. Kandwal, et al., "Statistical and spectral analysis of ECG signal towards achieving non-invasive blood glucose monitoring," *BMC Med. Inform. Decis. Mak.*, Vol. 19, 266, 2019.

23. Kandwal, A., T. Igbe, J. Li, et al., "Highly sensitive closed loop enclosed split ring biosensor with high field confinement for aqueous and blood-glucose measurements," *Sci. Rep.*, Vol. 10, 4081, 2020.

24. Tobore, I., A. Kandwal, J. Li, et al., "Towards adequate prediction of prediabetes using spatiotemporal ECG and EEG feature analysis and weight-based multi-model approach," *Knowledge-Based Systems*, Vol. 209, 106464, 2020.

25. Okoniewski, M., M. Mrozowski, and M. A. Stuchly, "Simple treatment of multi-term dispersion in FDTD," *IEEE Microwave and Guided Wave Letters*, Vol. 7, No. 5, 121–123, May 1997, doi: 10.1109/75.569723.

26. Tang, L., S. J. Chang, C.-J. Chen, and J.-T. Liu, "Non-invasive blood glucose monitoring technology: A review," *Sensors*, Vol. 20, No. 23, 6925, 2020.

27. Tang, W.-X., H. Zhao, J. Y. Chin, and T. J. Cui, "A meander line resonator to realize negative index materials," *2008 IEEE Antennas and Propagation Society International Symposium*, 1–4, 2008.

28. Keiser, G. R., H. R. Seren, A. C. Strikwerda, X. Zhang, and R. D. Averitt, "Structural control of metamaterial oscillator strength and electric field enhancement at terahertz frequencies," *Applied Physics Letters*, Vol. 105, 081112, 2014.

29. Mehrotra, P., B. Chatterjee, and S. Sen, "EM-wave biosensors: A review of RF, microwave, mm-wave and optical sensing," *Sensors*, Vol. 19, No. 5, 1013, 2019.

30. Schmickl, S., T. Faseth, and H. Pretl, "An RF-energy harvester and IR-UWB transmitter for ultra-low-power battery-less biosensors," *IEEE Transactions on Circuits and Systems I: Regular Papers*, Vol. 67, No. 5, 1459–1468, 2020.

31. Ahmadivand, A., B. Gerislioglu, R. Ahuja, and Y. K. Mishra, "Terahertz plasmonics: The rise of toroidal metadevices towards immune biosensings," *Materials Today*, Vol. 32, 108–130, 2020.

32. Suwalak, R., C. Phongcharoenpanich, D. Torrungrueng, and M. Krairiksh, "Determination of dielectric property of construction material products using a novel RFID sensor," *Progress In Electromagnetics Research*, Vol. 130, 601–617, 2012.

33. Guillod, T., F. Kehl, and C. V. Hafner, "FEM-based method for the simulation of dielectric waveguide grating biosensors," *Progress In Electromagnetics Research*, Vol. 137, 565–583, 2013.

34. Caratelli, D., A. G. Yarovoy, A. Massaro, and A. Lay-Ekuakille, "Design and full-wave analysis of piezoelectric micro-needle antenna sensors for enhanced near-field detection of skin cancer," *Progress In Electromagnetics Research*, Vol. 125, 391–413, 2012.